

Title	A NOVEL PT-BASED CATHODE CATALYST DESIGN BY FIRST PRINCIPLES
Author(s)	Nakanishi, H
Citation	Annual Report of FY 2007, The Core University Program between Japan Society for the Promotion of Science (JSPS) and Vietnamese Academy of Science and Technology (VAST). p491-p.495
Issue Date	2008
oaire:version	VoR
URL	https://hdl.handle.net/11094/13097
DOI	
rights	
Note	

Osaka University Knowledge Archive : OUKA

<https://ir.library.osaka-u.ac.jp/>

Osaka University

A NOVEL Pt-BASED CATHODE CATALYST DESIGN BY FIRST PRINCIPLES

C. Escaño, H. Nakanishi and H. Kasai

Department of Precision Science and Technology and Applied Physics, Osaka University, Suita, Osaka 565-0871, Japan

ABSTRACT

Polymer Electrolyte Fuel Cell (PEFC) has been considered as an environmentally friendly alternative power generator because of its high-energy efficiency and zero-emission. Since commercial viability of PEFC is still farfetched owing to the high cost of platinum, the most active catalyst known so far, one promising way to make progress in this field is to develop a low-cost and efficient catalyst material. In this report, we introduce a novel system: Pt monolayer on Fe(001) which exhibits favorable catalytic properties than pure Pt based on spin-polarized density functional theory (DFT) calculations .

Potential energy curves for the reaction of Pt with O₂ as a function of O₂ center-of-mass distance from the platinum surface and O-O interatomic distance show that Pt monolayer on Fe(001) produces a combination of weaker O binding and lower activation barrier for O₂ dissociation. These characteristics are both beneficial for easier O₂ dissociation to produce adsorbed O and subsequent reactions of O with other surface specie: H⁺, towards a direct 4-e⁻ reduction process to produce H₂O. Local density of states (LDOS) at the Pt surface shows spin polarization of unfilled *d*_{zz} protruding perpendicularly out of surface, increasing *d*_{zz}-vacancy on the surface and thus enhancing Pt surface reactivity. Such enhancement of Pt surface reactivity by Fe(001) gives significant insight on the role of magnetization of Pt in the design of cathode catalyst with improved activity and with considerable Pt loading reduction.

KEYWORDS

cathode catalyst , Fe(001), first principles , O₂ dissociation, Pt monolayer , Pt surface reactivity

INTRODUCTION

Recently, Pt-alloy systems have been recognized as potential cathode catalysts. A class of Pt-based alloys which include PtM (M=transition metal) and the so-called NSA's or near surface alloys (i.e. overlayer or subsurface structures of Pt on non-noble metal) have exhibited relatively higher cathode activity for oxygen reduction reaction (ORR) than pure Pt [1-2]. Since, PtM are typically richer in Pt content than the NSAs, a promising approach to design alternative cathode catalyst is to consider the latter system. Taking advantage of the fact that the properties of thin layer of metal grown on top of another are folded by effects of the substrate, tailoring catalytic activity of Pt may then capitalize on such metal-substrate interaction. Spin resolved photoemission studies on thin Pt film on Fe(001) have shown ferromagnetic coupling of Pt to Fe as a result of Fe 3*d* -Pt 5*d* states interaction [3]. Herein, we considered an overlayer structure of Pt on a ferromagnetic material: Pt_{tML}/Fe(001). Stability assessment of the system employs a simple model which includes an estimate of surface composition based on Ruben et. al. surface segregation energy in transition-metal alloys database [4]. From here, we note

that Pt has sufficiently negative segregation energy on Fe(001) suggesting a stable elemental Pt overlayer on Fe(001). In such a stable system, we investigated the influence of Fe substrate on the electronic and magnetic properties of Pt and its consequent effect on dissociation and adsorption of O_2 .

MATERIALS AND METHODS

Spin-polarized DFT-based total energy calculations were performed using first principles simulation code Vienna *ab initio* simulation package (VASP) [5-6]. Ionic cores were described by PAW potentials [7] and the Kohn-Sham one-electron valence states were expanded in a basis of plane waves with kinetic energy cutoff of 400 eV. For the exchange correlation energy, the generalized gradient approximation (GGA) within the Perdew-Burke-Ernzerhof (PBE) functional [8,9] was employed. The large supercell of $5.74\text{\AA} \times 8.61\text{\AA} \times 25.83\text{\AA}$ containing three-layer ferromagnetic slab of bcc Fe(001) of 6 atoms per layer and monolayer of 6 Pt atoms pseudomorphically laid on top of Fe was constructed with 5 equivalent layers of vacuum corresponding to a distance of $\sim 15\text{\AA}$. Such large supercell was carefully chosen to avoid interactions of oxygen with neighboring supercells. Full geometry and structure optimization of system shows no lateral reconstruction and a negligible change in Fe interlayer distances, in excellent agreement with experimental findings [10]. In the optimized structure, the induced magnetic moment of $0.46\mu_B$ per Pt atom is in full accordance with the experimentally determined value of $\sim 0.50\mu_B$ for Pt atom on (001)Fe/Pt multilayers using x-ray magnetic circular dichroism (XMCD) [11] and the calculated magnetic moment for bulk Fe is in good agreement with the experimentally derived bulk value [12]. Since O and Pt have large mass difference [13,14] rendering large difference in time scales associated with surface relaxation and O_2 dissociation dynamics [15], slab relaxation was not accounted for in the calculations. The O_2 adsorption geometry adopted the hollow-bridge site-hollow (H-B-H) configuration as it is reported to be the most stable O adsorption configuration on Pt(001) [16]. Finally, O_2 was constrained to move in parallel orientation at distance Z above the Pt layer with O_2 center-of-mass fixed at the bridge site as shown in FIG. 1. Corresponding total energies for varying O_2 c.m. distance from the platinum layer, Z and for varying O-O inter-atomic distance, r were calculated.

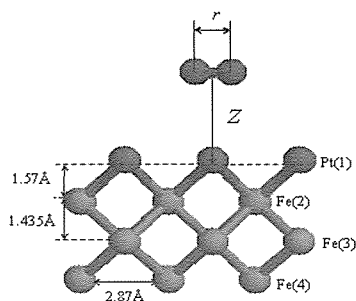


FIG.1 O_2 dissociative adsorption geometry

RESULTS AND DISCUSSION

The calculated potential energy for the reaction of Pt with O_2 as a function of the adsorbate-surface distance and O-O interatomic distance is shown in FIG. 2. Energies are given in electronvolts relative to the values at α configuration (equilibrium gas phase distance, $r = 1.21\text{\AA}$ and $Z=3.25\text{\AA}$) representing the distant O_2 . First potential energy curve (PEC) crossing between $r=1.20\text{\AA}$ and $r=1.40\text{\AA}$ is observed at $Z \approx 2.30\text{\AA}$ indicating O-O bond stretching to 1.40\AA from the gaseous O-O distance at 2.30\AA from the Pt layer. Next PEC crossing is observed at $1.5\text{\AA} < Z < 1.6\text{\AA}$ between $r=1.40\text{\AA}$ and $r=2.60\text{\AA}$ suggesting further elongation of O-O bond to 2.6\AA , a value comparable to O-O interatomic separation of 2.8\AA in Pt(001)[16]

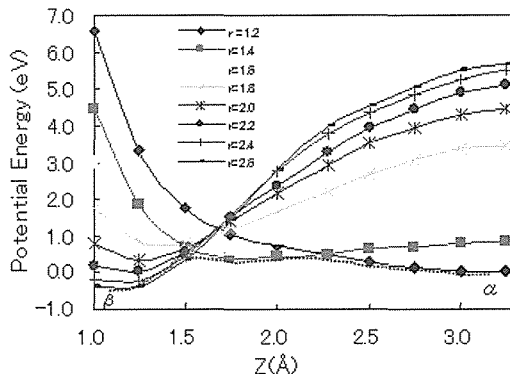


FIG.2 Potential energy as a function of r and Z , referenced to α configuration

which satisfies the condition of at least twice the equilibrium gas phase bond length O-O interatomic distance for O₂ to be completely separated. O₂ dissociation ends up at β where binding energy is -0.43 eV showing a less stable O adsorption compared to that of Pt(001). In the process of O₂ dissociation, O₂ encounters an activation barrier of 0.50 eV, just nearly half that of clean Pt(001), 1.2 eV [16].

Next, contour plots corresponding to the α and β configurations as shown in FIG. 3(a) and FIG. 3(b), respectively are compared. Charge density plots were taken on the plane depicted by the dashed line in the inset of FIG. 3(a) with corresponding contour spacing of 0.1 electrons/Å³. Since O and Pt atoms are not in such the same plane, we show in FIG. 3(b) inset, the charge density plot at other plane (at $\sim 51.0^\circ$ included angle with plane in (a)) to clearly view O-Pt bonding.

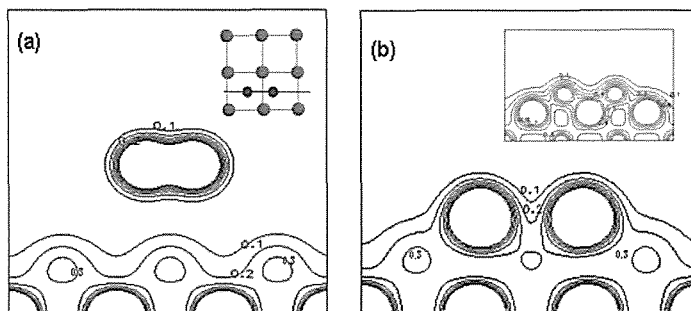


FIG.3 Charge distribution for (a) α and (b) β configurations

For (a), we observe a clear separation between electrons of O₂ and Pt surface while bonding between O atoms is much pronounced. On the other hand, upon O adsorption in (b), we note a clear separation in electron charge distribution around O atoms indicating marked separation of O atoms while bonds are being formed between O and neighboring Pt atoms as shown in the inset. Thus, as mentioned earlier, O₂ have completely separated on Pt monolayer on Fe(001) [17].

The lower activation barrier for O₂ dissociation can be associated to the enhancement of Pt surface reactivity upon Pt monolayer bonding to top Fe layer. Local density of states (LDOS) for clean Pt (FIG. 4(a)) and for Pt_{ML}/Fe(001) (FIG. 4(b)) indicate

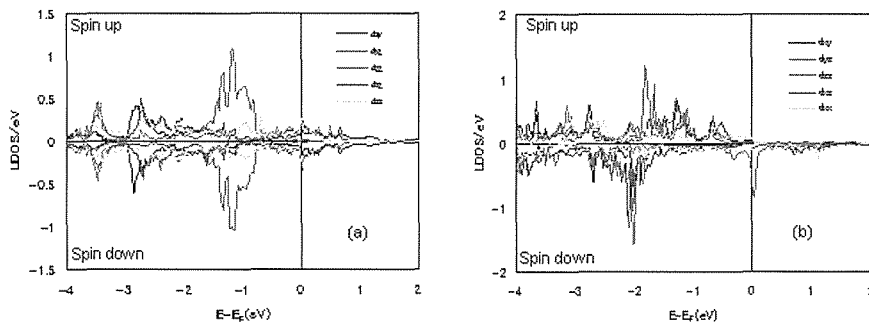


FIG.4 LDOS for (a) clean Pt (b) Pt_{ML}/Fe(001)

shifting of unfilled d_{zz} up the Fermi level (E_F) as characterized by spin polarization of d_{zz} at E_F increasing d_{zz} -vacancy in the surface. We think that d_{zz} orbital protruding perpendicularly out of the surface ensures sites for O₂-Pt interaction, thereby, increasing O₂ electron donation to Pt and enhancing facilitation of electron back donation to O anti-bonding orbital and hence, a O-O bond cleavage.

For the sake of further clarifying O-Pt interaction, we show in FIG. 5 the local magnetic moments and valence electron population of O, Pt and Fe before (α configuration) and after (β configuration) O is adsorbed. Atom index corresponds to an atom in a particular position as indicated in the inset of rightmost bottom panel. Significant decrease in magnetic moment of two separate oxygen atoms is seen indicating unpaired O electron donation to Pt surface, upon which the adsorbed O in turn induces appreciable reduction in Pt magnetic moment with a predominant decrease in 5th and 6th atoms by virtue of their positions as depicted in the inset figure. Such apparent decrease is associated with antiparallel spin alignment of O electron with Pt spin upon O adsorption. Considerable decrease in

magnetic moment extends to the first layer of Fe atoms. Same trend of interaction is shown by the changes in valence-electrons populations within the O, Pt and Fe-Wigner Seitz radii for the same configurations described earlier as depicted in the bottom panels of FIG. 5. Again there is a noticeable charge transfer from O₂ to the Pt surface as shown by a marked decrease in number of valence-electrons within the O-atom region. Consequently, an increase in valence-electrons populations within the Pt-atom region is observed with apparent increase in the 5th and 6th Pt atoms. Similarly, considerable change in number of valence-electrons extends to the first layer of Fe atoms.

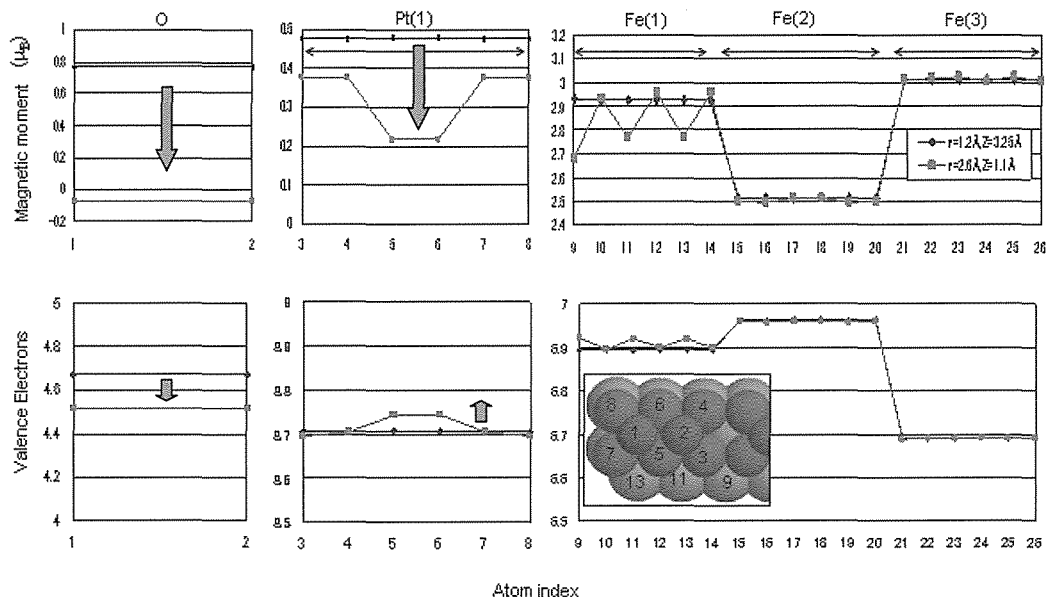


FIG.5 Local magnetic moments and valence electrons for O, Pt and Fe atoms before and after O is adsorbed.

CONCLUSIONS

Pt_{ML}/Fe(001) produces a combination of weaker O binding and easier O₂ dissociation than clean Pt which are both beneficial to produce adsorbed O and for easier subsequent reactions steps. Lower activation barrier for O₂ dissociation is ascribed to enhancement of Pt surface reactivity marked by increase d_{zz} -vacancy on the surface. The spin polarization of unfilled d_{zz} ensuring a sites for O₂-Pt interaction, thereby, increasing O₂ electron donation to Pt surface and weakening of O-O bond. Induced magnetic moment on Pt layer has provided consequent modification on Pt surface reactivity allowing easier O₂ dissociative adsorption. This introduces the role of magnetization of Pt in design of economically feasible cathode catalyst with improved catalytic properties.

ACKNOWLEDGMENT

This work is supported by the Ministry of Education, Culture, Sports, Science and Technology of Japan (MEXT) through their Grants-in-Aid for Scientific Research on Priority Areas (Developing Next Generation Quantum Simulators and Quantum-Based Design Techniques), Special Coordination Funds for the 21st Century Center of Excellence (COE) program (G18) “Core Research and Advance Education Center for Materials Science and Nano-Engineering” and Grants-in-Aid for Scientific Research supported by Japan Society for the Promotion of Science (JSPS). Some of the calculations

were done using computer facilities of the ISSP Super Computer Center (University of Tokyo), the Yukawa Institute (Kyoto University) and the Japan Atomic Energy Research Institute (ITBL, JAERI).

REFERENCES

- [1] T. Toda, H. Igarashi, H. Uchida, and M. Watanabe, *J. Electrochem. Soc.* **146**, 3750 (1999).
- [2] J. Zhang, Y. Mo, M.B. Vukmirovic, R. Klie, K. Sasaki, R. R. Adzic. *J. Phys. Chem. B* **108**, 10955-10964 (2004).
- [3] R. Bertacco and F. Ciccacci, *Phys. Rev. B* **57**, 96 (1997).
- [4] A.V. Ruban, H.L. Skriver and J.K. Nørskov. *Phys. Rev. B* **59**, 15990-16000 (1999)
- [5] G. Kresse and J. Furthmüller, *Comput. Mater. Sci.* **6**, 15 (1996).
- [6] G. Kresse and J. Furthmüller, *Phys. Rev. B* **54**, 11169 (1996).
- [7] G. Kresse and J. Hafner, *Phys. Rev. B* **47**, 558 (1993).
- [8] G. Kresse and J. Hafner, *Phys. Rev. B* **49**, 14251 (1994).
- [9] P.E. Blöchl, *Phys. Rev. B* **50**, 17953 (1994).
- [10] G. W. R. Leibbrandt, R. Van Wijk, and F.H.P.M. Habraken, *Phys. Rev. B* **47**, 6630 (1992).
- [11] W. J. Antel Jr., M.M. Schiwickert, Tao Lin, W.L. O'Brien and G.R. Harp, *Phys. Rev. B* **60**, 12933 (1999).
- [12] J. Lyubina, I. Opahle, M. Richter, O.Gutfleisch, K. Müller and L. Schultz, *Appl. Phys. Lett.* **89**, 032505 (2006).
- [13] A. Eichler, G. Kresse and J. Hafner, *Surf. Sci.* **397**,116 (1998).
- [14] B. Hammer and J.K. Nørskov, *Surf. Sci.* **343**,211 (1995).
- [15] A. Eichler, G. Kresse and J. Hafner, *Surf. Sci.* **397**,116 (1998).
- [16] S. Yotsuhashi, Y. Yamada, W. Diño, H. Nakanishi and H. Kasai, *Phys. Rev. B* **72**, 033415 (2005).
- [17] C. Escaño, T. Kishi, S.Kunikata, H. Nakanishi, H. Kasai. *J. Chem. Phys.* (submitted)